ECOGRAPHY

Research article

Decomposing biodiversity change to processes of extinction, colonization, and recurrence across scales

François Leroy◉✉[1], **Jiří Reif**◉[2,3], **Zdeněk Vermouzek**[4], **Karel Šťastný**[5], **Eva Trávníčková**[1,6], **Vladimír Bejček**[5], **Ivan Mikuláš**[4] and **Petr Keil**[1]

[1]Department of Spatial Sciences, Faculty of Environmental Sciences, Czech University of Life Sciences Prague, Praha-Suchdol, Czech Republic
[2]Institute for Environmental Studies, Faculty of Science, Charles University, Prague, Czechia
[3]Department of Zoology, Faculty of Science, Palacky University, Olomouc, Czechia
[4]Czech Society for Ornithology, Prague, Czechia
[5]Department of Ecology, Faculty of Environmental Sciences, Czech University of Life Sciences Prague, Praha-Suchdol, Czech Republic
[6]Department of Zoology, Faculty of Science, Charles University, Praha, Czech Republic

Correspondence: François Leroy (**francois.libert.leroy@gmail.com**)

Temporal biodiversity change involves colonization, extinction, and recurrence of species. These processes vary with spatial grain (i.e. the area at which biodiversity is assessed), but there is little theory to explain this. Here, we present theoretical scenarios showing that colonization, extinction, and recurrence of species can either increase or decrease in strength across grain size. We tested for these patterns in empirical data on Czech birds over 30 years, and several orders of magnitude of spatial grain. We found that colonization increased from local to national scales, while extinctions followed a hump-shaped pattern, leading to a higher temporal increase of richness towards coarse grains. Probabilities of colonization and extinction decreased with grain size, with a steeper decrease for extinction. Our results hold independently across two time periods (1985–2002 and 2002–2017), and colonization is the dominant process behind temporal change of richness. This decomposition of biodiversity change allowed us to identify scale-wise ecological mechanisms driving biodiversity change, and explain seemingly confusing directions of biodiversity change at different spatial scales.

Keywords: Anthropocene, bird atlas, breeding bird survey, extirpation, invasion, Jaccard, machine learning, persistence, presence–absence, range contraction, species–area relationship

Introduction

Biodiversity is under pressure, mostly from human activities (Pereira et al. 2012, Wilting et al. 2017, Harfoot et al. 2021). Consequently, global species pools and abundances in some taxa have been decreasing, triggering concerns that we may be in the midst of a sixth mass extinction (Barnosky et al. 2011, Ceballos et al. 2020).

www.ecography.org

However, recent studies reveal a surprising variability in temporal trends of biodiversity, which includes decreases, increases, and stability (Keil et al. 2011, Vellend et al. 2013, Dornelas et al. 2014, McGill et al. 2015, Schipper et al. 2016, Cardinale et al. 2018, Blowes et al. 2019, Finderup Nielsen et al. 2019, Leroy et al. 2023a), resulting in a confused message to decision makers and the public (Vaidyanathan 2021). Apart from data gaps and biases (Meyer et al. 2015), a major suspect behind the reported variability of biodiversity trends is variation in *spatial grain*, i.e. the area at which biodiversity is assessed (Jarzyna and Jetz 2018, Chase et al. 2019). This is because the relative strength of ecological processes can vary with spatial grain, which then affects the direction and magnitude of biodiversity trends (Sax and Gaines 2003). However, empirical assessment of cross-scale trends of biodiversity remains challenging due to lack of high-quality datasets from multiple spatial grains.

Among various facets of biodiversity, species richness (*S*) is the most fundamental and simplest metric: it is easy to assess, it has well-developed scaling theory behind it (Arrhenius 1921, Preston 1960, Adler and Lauenroth 2003, Storch et al. 2007, Storch 2016, McGlinn et al. 2019) and most other metrics either correlate with it, or they directly use *S* in their formula (e.g. Shannon's or Simpson's diversity indices). This makes the relationship between spatial grain and *S*, and between spatial grain and *temporal change of S* (hereafter ΔS) of particular interest. The three components of ΔS are colonization, extinction, and recurrence of species (Fig. 1), and these are also key components of metrics of temporal biodiversity turnover such as Jaccard index (Dornelas et al. 2014). ΔS has been shown to be grain-dependent (Jarzyna and Jetz 2018, Chase et al. 2019), but little is known about

how the spatial scaling of colonization, extinction, and recurrence combine to affect the spatial scaling of ΔS and temporal turnover. Even though Jarzyna et al. (2015) empirically show that probabilities of colonization, extinction, and temporal turnover decrease with spatial grain, we are unaware of any studies linking the scaling of those processes with the scaling of ΔS.

Here, we address this by, first, showing how ΔS is driven by colonization, extinction, and recurrence, and we present theoretical scenarios of how they play out across spatial grains. Second, we empirically assess more than 30 years of ΔS and rates of colonization, extinction, and recurrence across six orders of magnitude of spatial grains, from grain as small as 30 000 m², to thousands of km². We do this using data on birds in Czechia, a central European country with one of the best cross-scale datasets in the world. Specifically, Czechia has a monitoring scheme running for 40 years with hundreds of local ornithological routes surveyed. This dataset is complemented by independently surveyed high-quality, temporally replicated bird atlases of *ca* 10 × 10 km grain, surveyed across more than 30 years. These data offer a rare glimpse into dynamics of biodiversity that others examined either only at local grain (Dornelas et al. 2014, Blowes et al. 2019), or at larger grains such as regional, national, continental or global scales (Butchart et al. 2004).

We show that, for a given area *A*, the average trend of species richness change (hereafter $\overline{\Delta S}$, where the bar indicates the median change for a given area *A*) starts from zero at local grains and becomes positive with increasing spatial grain for birds of Czechia. This relationship between $\overline{\Delta S}$ and spatial grain *A* (hereafter the $\overline{\Delta S}$–area relationship) is upwards accelerating in a semi-log space, even for different temporal coverages. We

(a)

Extinction
E

Recurrence
R

Colonization
C

S_{time_1} S_{time_2}

(b)

Time 1   Time 2

$R = 2$

$E = 2$

$C = 1$

$S_{time_1} = E + R = 4$ $S_{time_2} = C + R = 3$

$$\Rightarrow \Delta S = S_{time_2} - S_{time_1} = C - E = -1$$

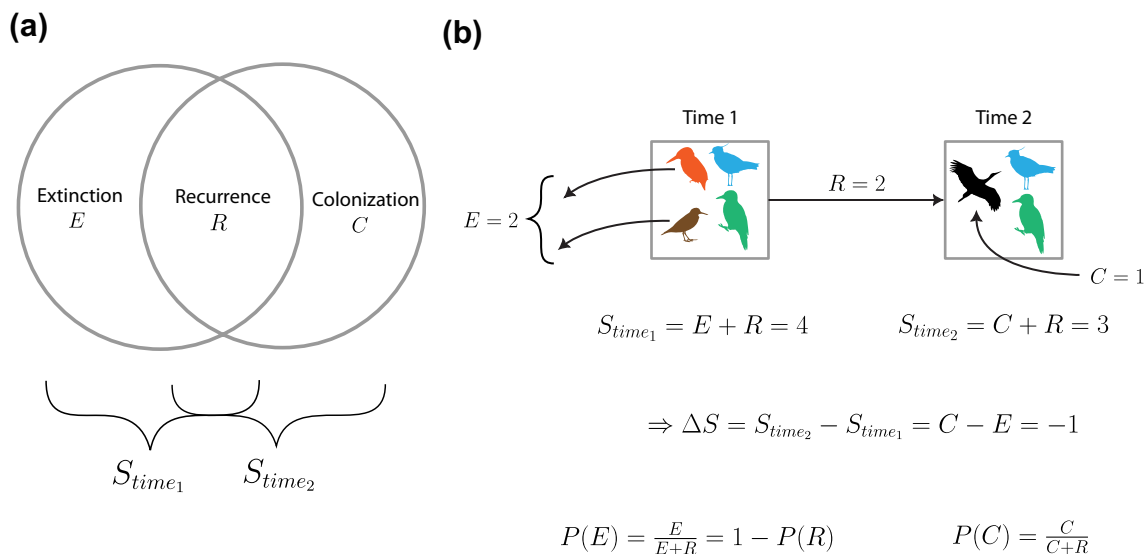$$P(E) = \frac{E}{E+R} = 1 - P(R) \qquad P(C) = \frac{C}{C+R}$$

Figure 1. (a) Communities at Time 1 and Time 2 share common species (i.e. number of recurrent species, *R*) but they also have species present at either Time 1 or Time 2 (i.e. *E*, the number of extinct species, and *C*, the number of species that have colonized the area, respectively). (b) Species richness at Time 1 and Time 2 (i.e. S_{time_1} and S_{time_2}, respectively) is composed of these three processes. Conversely, temporal changes of species richness (ΔS) can be decomposed to colonization (*C*), extinction (*E*), and recurrence (*R*) of species. Finally, *C*, *E* and *R* can be used to compute the probabilities of colonization *P(C)*, extinction *P(E)*, and recurrence *P(R)*.

show that this spatial scaling of $\overline{\Delta S}$ is caused by the spatial scaling of colonization, and extinction. Specifically, we show that colonization and extinction have the same values at local scales, but colonization is constantly increasing toward national scale while extinction displays a hump-shaped pattern, with lower values at both local and national scales. Linking the empirical scaling of extinction to our theoretical expectations, we explain the scaling pattern of extinction by a decline of common species and extinction of rare species. We also explain the scaling pattern of colonization by the arrival of newcoming species to Czechia. Finally, we show that the scaling intensity of extinction is robust to variation in time, and that colonization is the main driver of the shape of the $\overline{\Delta S}$ scaling.

Theory and expectations

In this section we define all the key components of species richness change (ΔS). We then explore several ecologically plausible scenarios, and the resulting expected spatial scaling of the components of biodiversity change.

Components of ΔS: colonization, extinction and recurrence

Considering an area A monitored at two points in time, the number of species S (i.e. species richness) at Time 1 (S_{time_1}) and Time 2 (S_{time_2}) can be expressed as the combination of 1) number of species present at both Time 1 and Time 2 (recurrence R, Fig. 1a), 2) number of species that colonized the area between Time 1 and Time 2 (colonization C) and 3) number of species that disappeared from the area between Time 1 and Time 2 (extinction E). The temporal change of species richness, ΔS, is then (Fig. 1b):

$$\Delta S = S_{\text{time}_2} - S_{\text{time}_1} = C + R - \left(E + R \right) = C - E \qquad (1)$$

Colonization, extinction, and recurrence can be assessed either as a count per unit of area A (e.g. the number of species that either colonized, went extinct or persisted through time, Fig. 1) or as probability (i.e. frequency). That is, we assume that the absolute values of C, E and R, depend on the number of species present and thus on the area A considered (through the species–area relationship, May 1975, Arrhenius 1921, Adler and Lauenroth 2003). Thus, from C, E and R, we compute the average per-species probabilities of colonization $P(C)$, extinction $P(E)$ (Keil et al. 2018) and recurrence $P(R)$:

$$P\left(C \right) = \frac{C}{C + R} \qquad (2)$$

which represents the frequency of colonizers (i.e. probability of a species present at Time 2 being a colonizer),

$$P\left(E \right) = \frac{E}{E + R} \qquad (3)$$

which is the frequency of a species going extinct (i.e. probability of a species present at Time 1 to go extinct and be absent at Time 2) and

$$P\left(R \right) = \frac{R}{E + R} = 1 - P\left(E \right) \qquad (4)$$

which is the frequency of species that persist from Time 1 to Time 2 (i.e. the probability of a species present at Time 1 to persist to Time 2). Note that $P(C)$ (Eq. 2) is different from the probability of a species not present at Time 1 (i.e. species from the species pool) to colonize the area (Supporting information). However, for the sake of simplicity, in the remainder of the manuscript we will use the expression 'probability of colonization' to refer to the values of $P(C)$ computed from Eq. 2.

We used simulations in order to better understand the relationship of the difference between C and E (Eq. 1), and the difference between $P(C)$ and $P(E)$. In these simulations, we used 8000 combinations of values of C, E, and R ranging from 1 to 1000 and we demonstrate (Fig. 1, Supporting information):

$$\text{sgn}\left[P\left(C \right) - P\left(E \right) \right] = \text{sgn}\left(C - E \right) = \text{sgn}\left(\Delta S \right) \qquad (5)$$

It means that diversity change over time has the same sign irrespective of whether extinctions and colonizations are measured as probabilities or as counts. This is encouraging because we can compare, at least qualitatively, studies that use these different measures of colonization and extinctions.

Importantly, C, E and R are also components of temporal turnover, for example the temporal *Jaccard's* similarity index:

$$\beta_j = \frac{R}{R + C + E} \qquad (6)$$

For any given spatial grain A in km^2, we will use bar sign to indicate median value of those metrics for a given grain A: $\overline{\Delta S}_A$ (read as "average species richness change for an area A"), $\overline{C}_A$, $\overline{E}_A$, $\overline{R}_A$, $\overline{P}\left(E \right)_A$, $\overline{P}\left(C \right)_A$, $\overline{P}\left(R \right)_A$ and $\overline{\beta_j}_A$.

Spatial scaling scenarios of processes behind richness change

In this section we show how different spatial scaling of $\overline{C}$, $\overline{E}$ and their respective probabilities $\overline{P}\left(C \right)$ and $\overline{P}\left(E \right)$ emerge from four hypothetical scenarios of re-arrangement of species composition within a region. We also show how the scaling of those processes combine into the scaling of $\overline{\Delta S}$. These scenarios do not represent all possible mechanisms involved in the scaling. Rather, they are mechanistic examples based on ecologically plausible processes observed in nature, proving that any of the given directions of spatial scaling (i.e. increasing or decreasing values of $\overline{C}$, $\overline{E}$, $\overline{P}\left(C \right)$ and $\overline{P}\left(E \right)$ with increasing grain A) are possible, biologically credible, and we can thus expect any of them in empirical data.

Scenario 1 (*Fig. 2a*) – extinction of rare species

This scenario shows that the number and per-species probability of extinction ($\bar{E}$ and $\bar{P}(E)$) can increase with increasing spatial grain A. Specifically, two rare species (i.e. blue and orange species with a restricted range and present in few grid cells at Time 1) go completely extinct at Time 2 whilst the occupancy of the widespread species remains constant, leading to an increased extinction towards coarse grain. In contrast, the scaling patterns of the number and per-species recurrence ($\bar{R}$ and $\bar{P}(R)$) decrease with increasing grain size (following Eq. 4, Fig. 1).

Scenario 2 (*Fig. 2b*) – decline of common species

This scenario illustrates that $\bar{E}$ and $\bar{P}(E)$ can decrease with increasing grain. Here, occupancy of the widespread species

(i.e. green bird) declines through time but does not reach 0, leading to a decrease of extinction towards large grain, as well as an increase of recurrence towards large grain.

Scenarios 1 and 2 have also been outlined for extinction in Keil et al. (2018). Here, we added the recurrence, and we also present two new scenarios leading to the opposite spatial scaling of colonization:

Scenario 3 (*Fig. 2c*) – spread of resident species

Here, the average number and probability of colonization ($\bar{C}$ and $\bar{P}(C)$) decrease with increasing grain, as local species already present in the large cell at Time 1 expand their occupancy (i.e. colonize new areas). Thus, colonization is null at the large grain (i.e. no new species colonize the large cell) and is higher at fine grain.
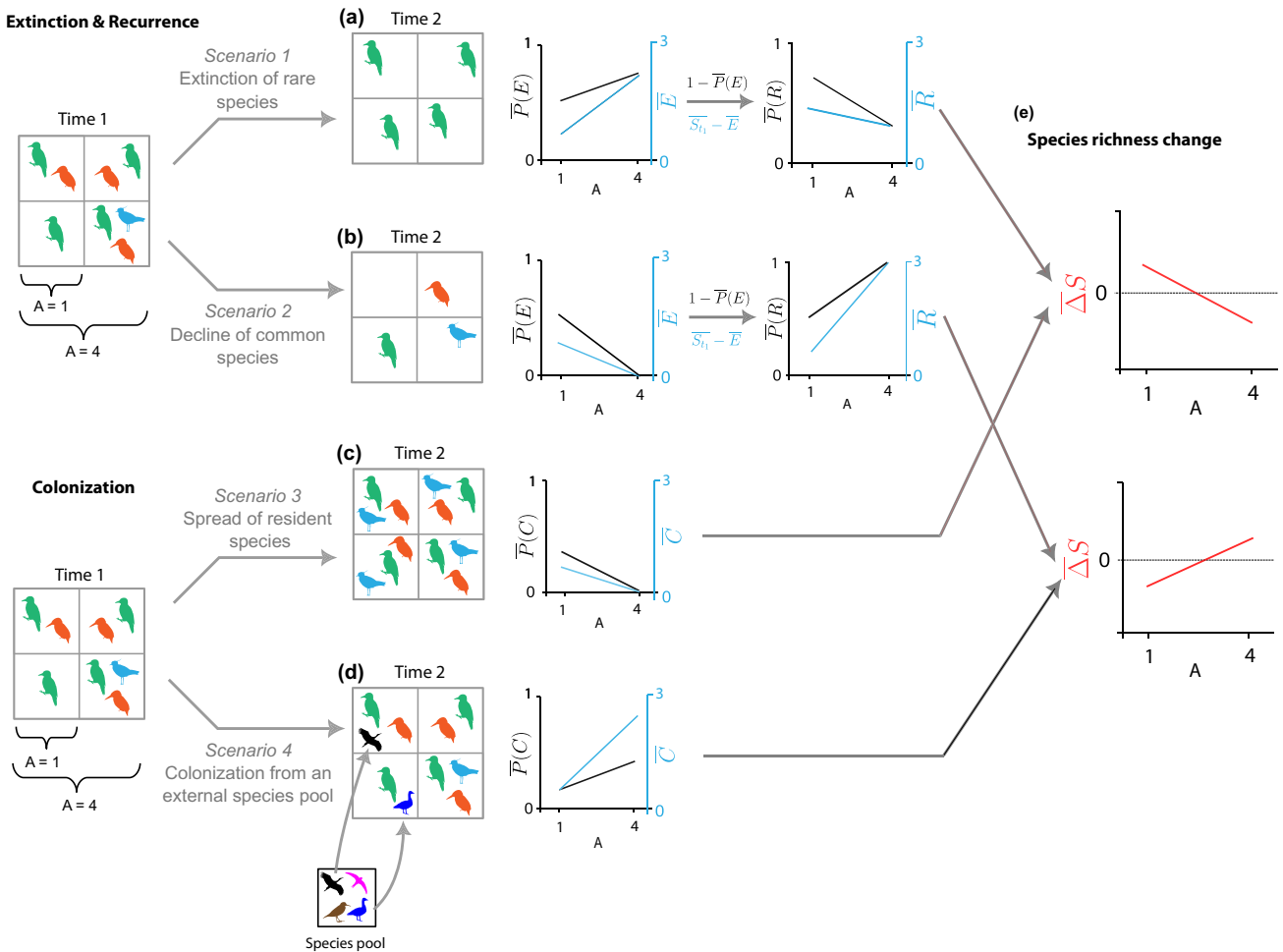

Figure 2. Conceptual diagrams of four different scenarios for the three components of ΔS (i.e. extinction E, recurrence R, and colonization C) and their probabilities (i.e. $P(E)$, $P(R)$, and $P(C)$, respectively). Using the same community compositions at Time 1 and two grain sizes (i.e. $A = 1$ and $A = 4$), we hypothesize how a rearrangement of a community through time (i.e. from Time 1 to Time 2) can lead to different scaling of extinction, recurrence, and colonization. The counts and probabilities for $A = 1$ are averaged over the 4 grid cells and this is represented by a bar (e.g. $\bar{C}$). The average number of events is represented in blue and the average probabilities in black. (a) Scenario 1 and (b) Scenario 2 show positive and negative scaling (respectively) of extinction (i.e. they are either (a) increasing or (b) decreasing with grain size) and the scaling of recurrence. (c) Scenario 3 and (d) Scenario 4 show different spatial scaling for colonization (i.e. decreasing and increasing, respectively). (e) Finally, we show how the scaling of colonization and extinction combine to the scaling of richness change ($\bar{\Delta S}$).

Scenario 4 (Fig. 2d) – colonization from an external species pool

In this scenario, $\bar{C}$ and $\bar{P}(C)$ increase with spatial grain A. For this to be possible, we need to consider non-native species from the species pool (i.e. species that are absent at Time 1 in the large cell). As each non-native species colonizes only one small cell, the large cell is a subject of all these colonizations, leading to an increasing colonization towards large grain.

Combining those different scaling scenarios of colonization and extinction then leads to distinct spatial scaling of $\overline{\Delta S}$ (Fig. 2e, Eq. 1, 5).

Material and methods

Czech bird datasets

To empirically assess avian biodiversity changes across spatial scales, we used the following two avian datasets from Czechia representing a large range of spatial grains spanning several orders of magnitude (from 30 000 m² to ca 80 000 km², the latter being the entire area of Czechia).

First, we used the three 'Czech breeding bird atlases' (hereafter CzAtlas, Šťastný et al. 1997, 2006, 2021) which represent the coarsest spatial grains. The first atlas covers the period of 1985–1989, the second 2001–2003 and the third one 2014–2017. The atlases use a grid resolution of approx. 10 × 10 km. Each grid cell is assigned one or several volunteers in charge of recording the species throughout the periods covered. We spatially aggregated the grid cells and biodiversity data into 20 × 20, 40 × 40 km and into one cell for the entire Czechia (ca 83 900 km², gridded maps of Fig. 3c). All together, those three atlases represent cumulative work of ca 2000 volunteers over more than 30 years aggregating more than a million incidences of 241 species.

Second, we used the 'Czech Breeding Bird Survey' (hereafter CzBBS, Reif et al. 2013), which represents fine (i.e. local) spatial grains. This has been an ongoing yearly monitoring program established in 1982, and it is similar to the North-American BBS (Sauer et al. 2017). CzBBS data are collected twice a year along a total of 350 transects of different shape and size spread across Czechia. Each transect is divided to 20 points where volunteers count birds under a standard protocol. Thus, the CzBBS represents two different spatial grains: the point grain and the transect grain (i.e. merging the 20 points). By cumulating all the censuses from 1982 to 2020 together, the CzBBS represents more than 1 million incidences of 236 species gathered over almost 40 years by more than 200 volunteers. In order to compare the CzBBS to the CzAtlas, we filtered the censuses of the CzBBS for the years corresponding to the CzAtlas periods (i.e. 1985–1989, 2001–2003 and 2014–2017).

Accounting for biases using machine learning (ML)

Both datasets have biases that we need to account for to make things comparable. In CzAtlas, there are different temporal spans of the three periods (i.e. the different duration of the census periods which are 5, 3 and 4 years, respectively) and there are variations in the number of volunteers assigned to each grid cell (i.e. sampling effort). In CzBBS, data are missing for some transects and some years due to turnover of volunteers, and the shape of the transects is not constant, with some transects more elongated than others, which can affect species counts (Kunin 1997). Clearly, CzAtlas has different biases than CzBBS; thus, in each dataset, we took a slightly different path to account for these biases.

To statistically control for biases, we used a cross-scale machine learning framework (ML, details below, also see Keil and Chase 2019). In order to maximize performance of the ML, we fitted and compared three different tree-based ML algorithms (Supporting information) using repeated (n = 3) k folds cross validation (k = 10), specifically: 1) random forests (RF, Breiman 2001), 2) boosted regression trees (BRT, Friedman 2001) and 3) extreme gradient boosting (XGBoost, Chen and Guestrin 2016). Those tree-based ML algorithms have the advantage of being flexible by allowing linear and non-linear effects of predictors, as well as interactions between them, without specifying them a priori (Hastie et al. 2009). This can make them hard to interpret, but ideal for predictive modelling that we do here (Pichler and Hartig 2023).

RF, BRT and XGBoost were fitted using the packages ranger (Wright and Ziegler 2017), gbm (Greenwell et al. 2020), and xgboost (Chen et al. 2022), respectively. For each model, we report their respective explained variance (i.e. R^2) and root mean squared error (i.e. RMSE) in Supporting information. All analyses were conducted in R ver. 4.4.1 (www.r-project.org).

Response variables in each ML algorithm were 1) species richness (S), 2) numbers of colonization, extinction and recurrence (C, E and R), and 3) probabilities of colonization, extinction, and recurrence ($P(C)$, $P(E)$ and $P(R)$, Supporting information).

Predictors that were common to all the response variables were latitude, longitude, elevation, and grain area (Supporting information). We also accounted for the elongation of the spatial units (i.e. shape of the transects, grid cells, census points…) using the following predictor:

$$\text{Elongation} = \frac{A_{\text{hull}}}{\sum_i^n A_{\text{units}}} \tag{7}$$

where A_{hull} is the area of the convex hull fitted around the unit of area, and $\sum_i^n A_{\text{units}}$ is the summed area of the n sub-units of A_{hull} (e.g. for the transects of the CzBBS, A_{hull} is the area of the convex hull of the transect and $\sum_i^n A_{\text{units}}$ is the summed area of the 20 census points). Thus, a squared or circular area would have a higher value than a narrow rectangle or an ellipse. These predictors represent the spatio-temporal
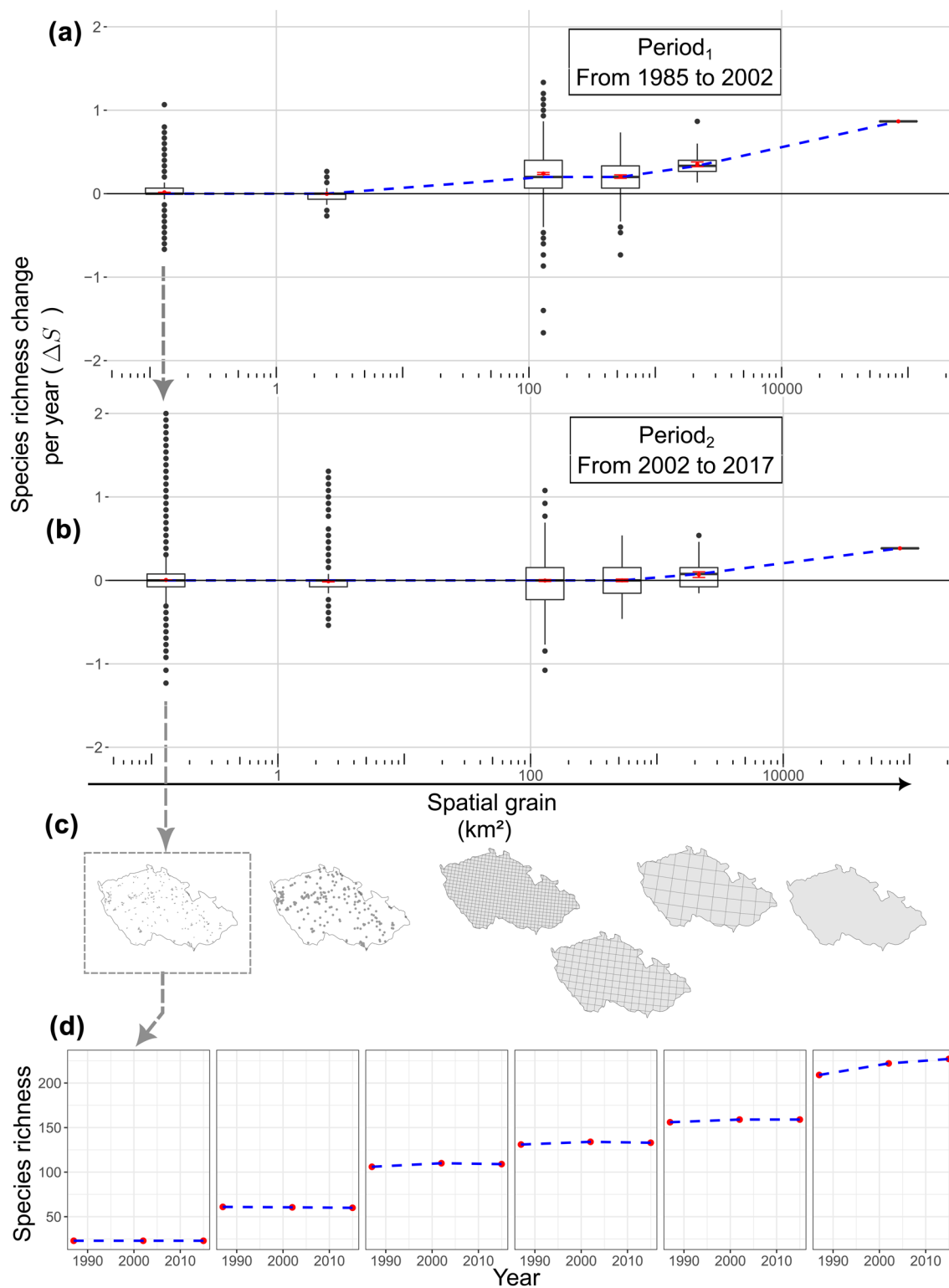
Figure 3. Predicted temporal trends of avian species richness (ΔS) with increasing spatial grain from (a) 1985 to 2002 (period$_1$), and (b) 2002 to 2017 (period$_2$). Each box in (a) and (b) represents the median species richness change (bound by the blue dotted line) and quartiles Q1 and Q3. The red dot and bars represent the mean and standard error. The spatial grain of each box in (a)–(b) and each panel in (d) is represented by a map in (c) (from <1 km² to entire Czechia). The average temporal trend at each spatial grain is shown in (d), where each red dot is the mean predicted species richness bound by the dotted blue lines (representing $\overline{\Delta S}$).

context of the data, and allow the ML to be interpolated and to predict the response at any desired location in space, location in time, spatial grain, and temporal grain (Keil and Chase 2019, 2022).

For the CzAtlas we used the number of observers per grid cell and per sampling period as a predictor representing the sampling effort. However, this was missing for the last period of the CzAtlas. In that case, we assumed a linear relationship between the temporal span and the number of observers for the two first time periods (i.e. five and three years, respectively) and predicted the sampling effort for a time span of four years (i.e. time span of the last atlas period).

Since C, E, R, $P(C)$, $P(E)$ and $P(R)$ have a temporal dimension, we modified some covariates for these responses (Supporting information). That is, instead of the temporal grain used to predict S, we used the log ratio of the temporal grain of the two periods considered. Also, we used the log ratio of the sampling effort between the two atlases considered. Finally, we used the period as a discrete predictor (i.e. whether between the two first atlas periods, from 1985 to 2002, or between the two last atlas periods, from 2002 to 2017).

Concerning the hyperparameters of the different algorithms, we set the number of trees to 500 for both RF and BRT and the minimum node size to five for RF, BRT and XGBoost. In the RF, we set the number of variables used for each split (i.e. 'mtry' argument) to one third of the number of covariates. For the BRT, we set the interaction depth to 1, and shrinkage to 0.1. For the XGBoost algorithm, we set the learning rate to 0.1, and the minimum loss reduction to 0 (Github repository for reproducible example, https://github.com/FrsLry/ms_scaling_changes, and released version on Zenodo https://doi.org/10.5281/zenodo.8432090).

For each response variable (i.e. S, C, E, R, $P(C)$, $P(E)$ and $P(R)$) and dataset (i.e. CzBBS or CzAtlas), we selected the model with the highest R^2 and lowest RMSE (Supporting information). The ML algorithms explained most variation in species richness (R^2(CzBBS) = 0.98, R^2(CzAtlas) = 0.77), less variation in the number of colonizations, extinctions and recurrences (R^2(CzBBS) = 0.56, R^2(CzAtlas) = 0.54), and the least variation for their respective probabilities (R^2(CzBBS) = 0.31, R^2(CzAtlas) = 0.40). Also, for each selected model, we checked for predictor correlations, and we assessed relative variable importance (Supporting information).

Predicting from the fitted ML models

We used the fitted ML models to predict S, C, E, R and their probabilities $P(C)$, $P(E)$ and $P(R)$ across the whole Czechia, at a sequence of spatial grains A (from 0.03 to ca 83 900 km^2), assuming a constant sampling protocol, and fixing the time-span to 4 years (i.e. the mean of the three atlas time spans). For each spatial grain of the CzAtlas, we set the sampling effort according to a quadratic linear regression of the sampling effort as a function of the spatial grain (Supporting information). We set the elongation index to 1 (Eq. 7). We used the latitude and longitude of the centroid of the convex hull, as well as the average elevation for each polygon. The CzAtlas had not covered every year of the CzBBS yearly dataset; thus, we set the dates of the predictions to the average year of each atlas (i.e. 1987, 2002, 2015). We then computed the similarity index following Eq. 6 using the output of those ML models.

Assessing ΔS for period$_1$ (1985–2002) and period$_2$ (2002–2017)

From the ML predictions, we assessed ΔS as the slope of a fitted simple linear regression between S and time:

$$S = \beta_0 + \Delta S \times t \qquad (8)$$

here t is the year and β_0 the intercept. Thus, ΔS is the average change of species number per year during the temporal extent. Following Eq. 1, ΔS in Eq. 8 is the average difference between colonization and extinction for the period considered.

We predicted ΔS for the two following periods: period$_1$, corresponding to the two first atlases, i.e. from 1985 to 2002 and period$_2$, corresponding to the second and third atlases, i.e. from 2002 to 2017. Period$_1$ and period$_2$ have almost the same temporal coverage (i.e. 17 and 15 years, respectively), and we thus consider the value of ΔS, C, E and R to be directly comparable.

Results

Spatial scaling of ΔS

We estimated ΔS in empirical time series of bird communities in Czechia, from local (ca 30 000 m^2) to national scales (ca 80 000 km^2), and within two time periods (period$_1$: 1985–2002, period$_2$: 2002–2017). For both periods and at fine spatial grains (i.e. $A = 0.03$ and $A = 2.51$ km^2), we found that $\Delta S_{0.03}$ and $\Delta S_{2.51}$ exhibited high variation and a zero median trend (i.e. Fig. 3a–b, d). The variation decreased towards coarser grains and $\overline{\Delta S}$ (i.e. the median value of ΔS) became positive with increasing grain (Fig. 3a–b, d). We also observed the same pattern for the overall temporal extent (i.e. from 1985 to 2017, Supporting information). Even though the shape of the $\overline{\Delta S}$–area relationship was similar across the two time periods, there were also some differences. Specifically, for period$_1$, $\overline{\Delta S}$ became higher than zero at a smaller spatial grain than for period$_2$ (i.e. for $A = 130$ km^2 and $A = 2170$ km^2, respectively). Second, from $A = 130$ km^2 up to entire Czechia, $\overline{\Delta S}$ for period$_1$ was always higher than $\overline{\Delta S}$ for period$_2$, meaning that the increase of S at any given grain size was higher during period$_1$ (Fig. 3d).

Spatial scaling of colonization, extinction, recurrence and turnover

We also estimated C, E, R and their respective probabilities $P(C)$, $P(E)$ and $P(R)$ across spatial grains for period$_1$
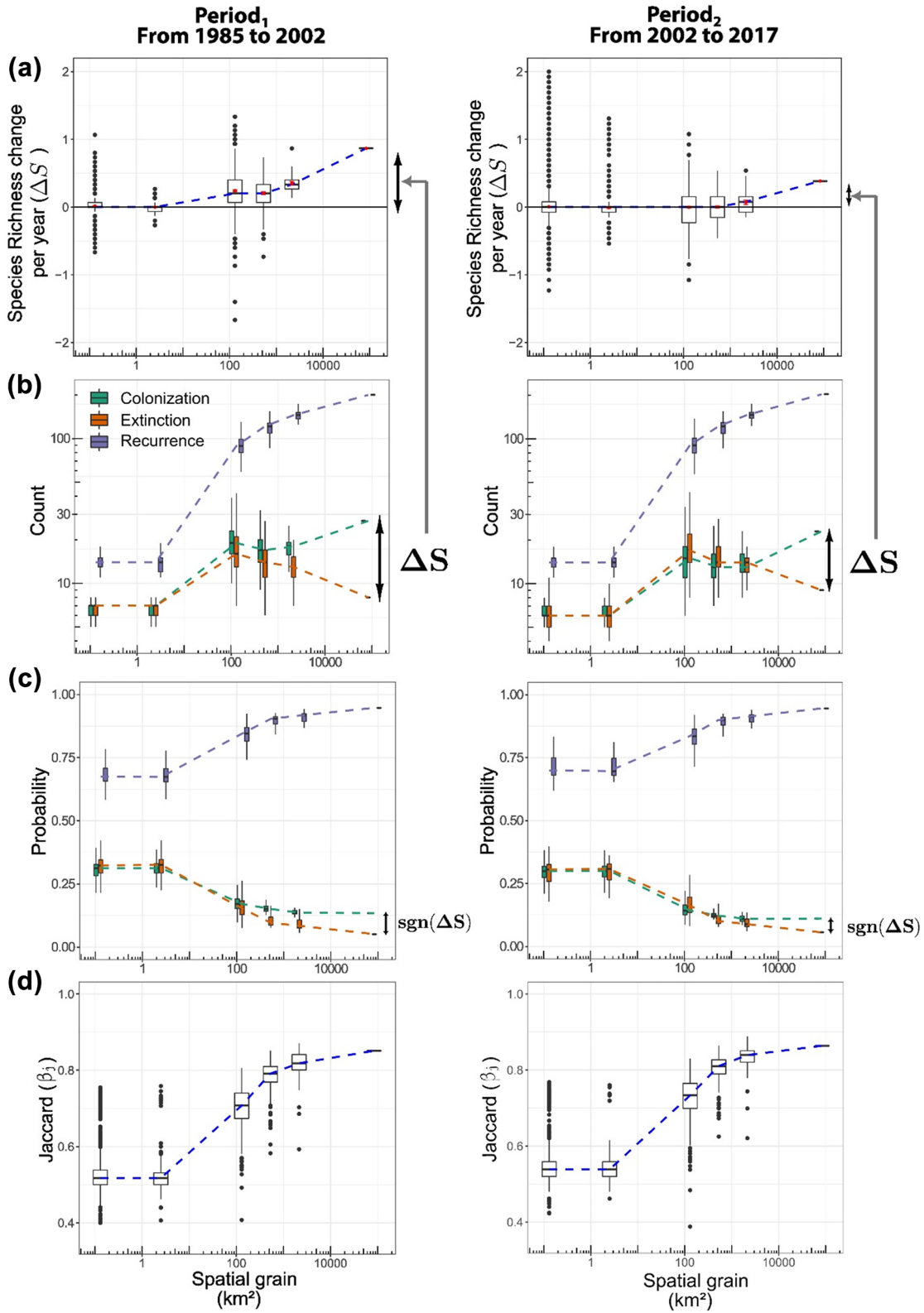
Figure 4. Boxplots showing the relationships of (a) the temporal trend of species richness (ΔS), (b) number of colonizations *C*, extinctions *E*, and recurrences *R*, (c) probabilities of colonization *P(C)*, extinction *P(E)*, recurrence *P(R)*, and (d) Jaccard similarity index β_j with increasing spatial grain for two time periods (i.e. period_1 left column, and period_2 right column). The spatial pattern in (a) (i.e. stronger positive $\overline{\Delta S}$ with increasing spatial grain) and (d) (i.e. increase of communities similarity with grain size) are driven by (b) and (c), the spatial scaling of colonization, extinction and their probabilities.

and period$_2$ (Fig. 4b–c). For both time periods, $\bar{C}$ and $\bar{R}$ increased with increasing grain while $\bar{E}$ increased until $A = 130$ km^2 and then decreased (Fig. 4b). Also, the difference between $\bar{C}$ and $\bar{E}$ increased with increasing grain (Fig. 4b) and this is reflected in the increasing ΔS–area relationship (Fig. 4a). In contrast, $\bar{P}(C)$ and $\bar{P}(E)$ both decreased with area, with a steeper decrease in $\bar{P}(E)$ (Fig. 4c). For the overall temporal extent, i.e. from 1985 to 2017, we found the same patterns (Supporting information). The Jaccard similarity index (i.e. turnover) β_j gradually increased from local to national grain (Fig. 4d).

Spatial scaling in period$_1$ vs period$_2$

Even though the sign of the scaling relationship was the same between period$_1$ and period$_2$ for all the processes

(Fig. 4), their magnitude differed (Fig. 5). The difference of $\overline{\Delta S}$ spatial scaling between the two time periods (Fig. 5a) arises at $A = 130$ km^2 and further increases towards coarser grains, with values of $\overline{\Delta S}$ higher in period$_1$. Indeed, $\overline{\Delta S}$ becomes visibly positive for period$_2$ only at the national scale. In the same way, the difference between $\bar{C}$ and $\bar{E}$ starts at $A = 130$ km^2 and further increases towards coarser grains for period$_1$, while this difference is only visible at the national scale for period$_2$ (Fig. 4b). Interestingly, the scaling of both $\bar{E}$ (Fig. 5e) and $\bar{P}(E)$ (Fig. 5f) was the same in both periods (also similar to the scaling for the overall temporal extent, 1985–2017). However, the scaling of both $\bar{C}$ (Fig. 5b) and $\bar{P}(C)$ (Fig. 5c) between period$_1$ and period$_2$ showed the same differences than for $\overline{\Delta S}$, with $\bar{C}$ and $\bar{P}(C)$ for period$_1$ higher than period$_2$ from $A = 130$ km^2 onward. Finally, concerning the temporal $\overline{\beta_j}$ similarity
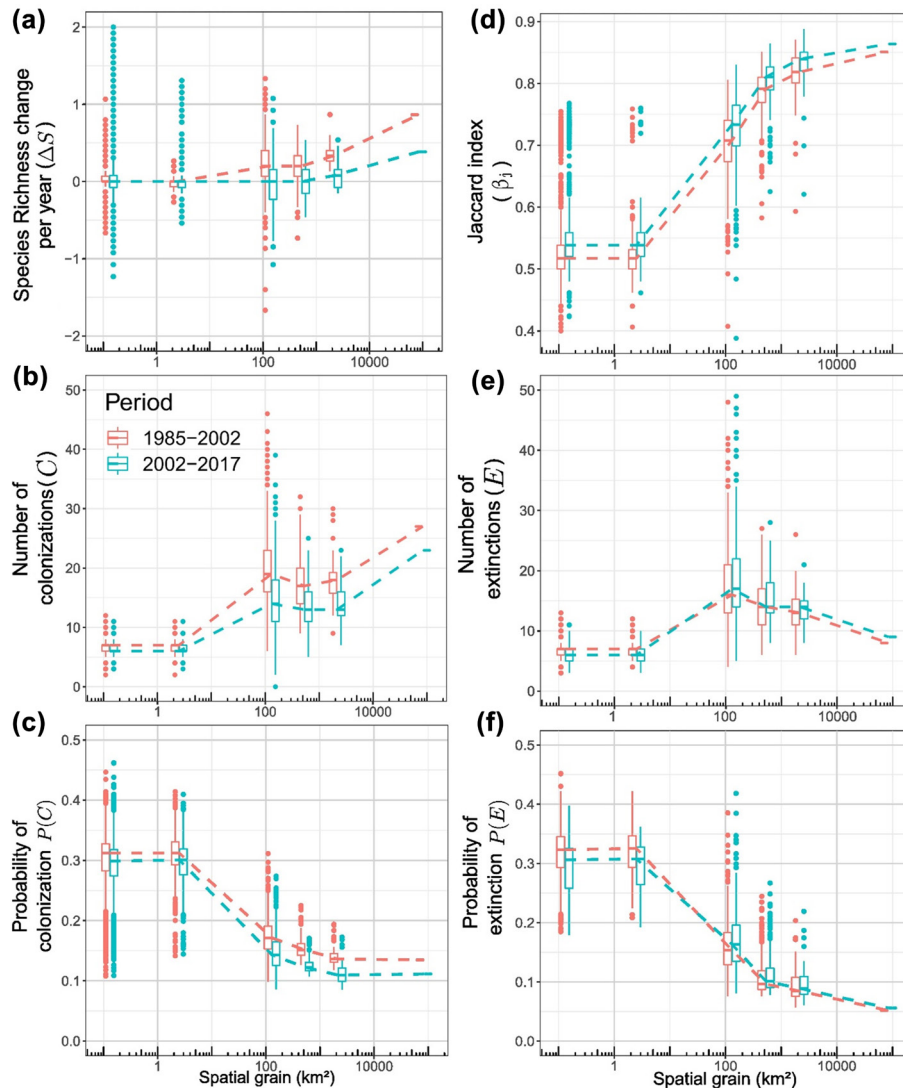

Figure 5. Comparison of the spatial scaling between period$_1$ (1985–2002; red) and period$_2$ (2002–2017; blue) of (a) species richness change ΔS, (b)–(c) number and probability of colonization, (d) Jaccard's temporal similarity index and, (e)–(f) number and probability of extinction.

index (Fig. 5d), its values for period$_2$ were always higher than for period$_1$.

Discussion

Spatial scaling of extinction and colonization

Our most important finding is the diverging scaling pattern of colonization and extinction for birds of Czechia: there is a positive relationship between grain size and the number of colonizations, which diverges from the hump-shaped relationship between grain size and the number of extinctions. This leads to no net average change of species richness at fine grains, but a net increase at coarser grains.

The increasing number of colonizations from local to national scale is consistent with the scenario of colonization by new species from an external species pool of bird species outside of Czechia (Fig. 2d – scenario 4), where the newcomers initially occupy a small fraction of the country. This pattern is often observed at initial stages of spread of non-native species (Wilson et al. 2004, Hastings et al. 2005). It only takes a single individual to make such a colonization event, which makes this positive scaling of colonization numbers with area a likely case. Example of species that follow this pattern in our dataset are the eastern imperial eagle *Aquila heliaca*, the wood duck *Aix sponsa*, the golden eagle *Aquila chrysaetos*, the cattle egret *Bubulcus ibis*, the whooper swan *Cygnus cygnus*, the egyptian goose *Alopochen aegyptiaca*, the barnacle goose *Branta leucopsis* or the citrine wagtail *Motacilla citreola*, also see Supporting information). In the future, we expect these colonizations to continue, as for landlocked Czechia, colonization can potentially come from four different countries (i.e. Germany, Poland, Slovakia, Austria) and the species pool is high (ca 600 breeding bird species in Europe, Keller et al. 2020). However, the dominant colonization source will probably be southern species due to ongoing climate warming which significantly shapes population trends of Czech birds (Storch et al. 2023). Indeed, some of the species in the examples above are of southern origin (Keller et al. 2020).

Unlike colonization, the scaling of extinction counts with area shows a hump-shaped pattern. Our theoretical scenarios (Fig. 2a–b – scenario 1–2) do not consider such a shape and only predict patterns of linearly increasing or decreasing scaling of extinction. Thus, to explain the observed pattern, we propose that both scenarios operate simultaneously, i.e. that range contractions occur both in common species at large scales (scenario 2, Fig. 2b) as well as in rare (but spatially sparse) species at local grain (scenario 1, Fig. 2a). A complementary explanation of this pattern is to combine the per-species probability of extinction in a given area (Fig. 4c, 5f) with the species–area relationship (Fig. 3 in ref. Keil et al. 2018). The number of extinctions results from the multiplication of the probability of extinction with the species–area relationship (SAR, Keil et al. 2018). Here, the probability of extinction is decreasing with area (Fig. 4c, 5f), which indicates a decline of common species (Fig. 2b, scenario 2, e.g. *Perdrix*

perdrix, Supporting information). This decline of probability of extinction, combined with a steep SAR reaching a plateau, result in the hump-shape pattern of the number of extinctions. This SAR shape is typical of the Czech ecosystems, with high alpha diversity and low gamma diversity (i.e. fields, forests, water pounds and city found close to each other and repeated all across the nation).

From counts to probabilities

Unlike counts, the average per-species probabilities of extinction $\bar{P}(E)$ and colonization $\bar{P}(C)$ exhibit a monotonically decreasing relationship with area, with a steeper decline of probability of extinction. The same relative scaling of $\bar{P}(C)$ and $\bar{P}(E)$ was observed for birds of the New-York state (Jarzyna et al. 2015). Theoretically, the decline of extinction probability with area is expected as larger areas harbor more species with larger populations, which are less likely to go extinct. In case of probability of colonization, its decline with area can be explained by the fact that the larger the area, the smaller the fraction of the pool of potential colonizers (since larger fraction of the species pool has already been included in the area), a mechanism involved in generating the colonization pattern according to the theory of island biogeography of MacArthur and Wilson (1967). Also, the increasing number of species with area increases the denominator when computing the probabilities (Eq. 2–3), leading to the decrease of probabilities (Eq. 2 and 3) Remarkably, we observed that counts of extinctions or colonizations follow a different scaling with area than their respective probabilities. This contrasts with our theoretical scenarios (Fig. 2) in which counts and probabilities always have the same sign of the scaling relationship. This is possible, as the shape of the species–area relationship creates a complex link between probabilities and numbers of events with increasing grain size (Keil et al. 2018).

From colonization and extinction to richness change

The abovementioned scaling of colonization, extinction and recurrence combine to a monotonically increasing spatial scaling of richness change $\overline{\Delta S}$. This increasing $\overline{\Delta S}$–area relationship (Fig. 2a–b) has been observed in other regions. Keil et al. (2011) describe it for British hoverflies, Jarzyna and Jetz (2018) and Chase et al. (2019) showed it for birds of the contiguous United-States. The only exceptions we found in the literature (i.e. decreasing $\overline{\Delta S}$ with grain) were for two closed systems, namely coral reefs and Hawaiian birds (Chase et al. 2019), where colonization at large grain are less likely due to substrate saturation and distance from the coast, respectively (MacArthur and Wilson 1967). Thus, empirical evidence so far suggests that the positive spatial scaling of $\overline{\Delta S}$ is the more likely pattern from local to regional grains in open continental ecosystems. However, speciation is most likely lower than the current extinction rates (Barnosky et al. 2011), which will ultimately push any ΔS–area relationship

to be negative as it approaches the global scale (Jarzyna and Jetz 2018). At first glance, our results of no net change (or an increase) of biodiversity do not align with studies reporting the global decline of biodiversity (Szabo et al. 2012). This is because the temporal trends of richness are grain dependent, and global decline is happening together with diverse trends at finer grains (Dornelas et al. 2014, 2023, Leroy et al. 2023a). We should keep in mind that most known extinctions in Europe happened before the temporal scope of this study, and so ecosystems may now be recovering from past perturbations (Cardinale et al. 2018) thanks to, e.g. conservation policies (Koschová et al. 2018). Also, short time series may be misleading if they end before an extinction debt is realized (Tilman 1994).

Temporal turnover

Even though the count of species recurrence (R) in time does not affect the scaling of $\overline{\Delta S}$, it is central in the scaling of temporal turnover Eq. 6. We showed that R increases with area faster than extinction or colonization rates, which then leads to the observed increasing temporal similarity (i.e. the Jaccard index β_j) with grain (Fig. 4d). We explain this by the structure of the Czech landscape, which exhibits high habitat heterogeneity (and species spatial turnover) at local grain but not at large grains (Keil et al. 2012). Thus, any fast temporal turnover at local grains caused by local stochasticity is likely asynchronous (because of local habitat heterogeneity) and dampens towards coarse grains where recurrence is high and all habitats are present. This pattern was also found for North-American birds (Jarzyna et al. 2015, Jarzyna and Jetz 2018). However, we could expect turnover to increase again if the grain considered is large enough to encompass different biomes (e.g. grain of the size of a continent), which would bring a large input of new species and make the link between turnover and grain triphasic (i.e. an increase, followed by a plateau, followed by another increase).

Generality through time

The scaling pattern of richness change, colonization, extinction, and temporal turnover showed the same directions when examined for 1985–2002 and for 2002–2017 (also for the overall time period 1985-2017, Supporting Information); this points to an encouraging constancy of the processes in time and indicates that our findings are general. However, Czech avifauna recovered intensively from 1985 to 2002 (Koleček et al. 2010) and this recovery probably slowed from 2002 to 2017. This pattern corresponds to the pattern of climatic changes in Czechia (Reif et al. 2021). Unlike extinction, the magnitude of the scaling of colonization varied between period$_1$ and period$_2$ (Fig. 5b–e), and this is driving the different scaling of richness change. That is, processes responsible for extinction did not change from 1985 to 2017 while the processes responsible for colonization decreased with time. We have reasons to think that the extinction rate was already

remarkably high in the 80's (Reif et al. 2021), and we show that there has been no improvements since the beginning of the 21st century neither at local nor national scales (Fig. 5e–f). On the other hand, decrease of colonization between the two time periods is a sign of the well-known spatial homogenization of avian communities (Devictor et al. 2008, Koleček et al. 2010, Davey et al. 2012, García-Navas et al. 2020, Reif et al. 2022), which is reflected by temporal turnover (Fig. 5d, higher temporal turnover for period$_1$ than for period$_2$).

Caveats

Assessing temporal trends of biodiversity across scales is challenging. Even though the performance of the cross-scale machine learning method we used is encouraging and may help assess biodiversity changes for data-poor regions (Keil and Chase 2019), we had to make weighty choices. Concerning the CzAtlas data, we accounted for the sampling effort by considering the number of observers assigned in each grid cell. However, no information was available on the actual counting time of each observer (i.e. temporal grain of the sampling plan, Leroy et al. 2023a). We couldn't harmonize the sampling effort of the CzAtlas with the sampling effort of the CzBBS (i.e. time spent at each census point/transect). This prevented us from fitting a single model for the two datasets together, which would have allowed us to predict biodiversity for missing spatio-temporal locations in between both datasets. Also, even though we adapted the CzBBS to the periods of the three CzAtlases (i.e. Atlas 1: 1985–1989; Atlas 2: 2001–2003; Atlas 3: 2014–2017), we warn that the sampling time at each point/transect of the CzBBS (i.e. temporal grain of the sampling) was different than the sampling time in each grid cell of the CzAtlas. Also, the modeling framework we used here did not correct for detection probability, which is nowadays often done with, e.g. using hierarchical occupancy models (MacKenzie et al. 2006, Kéry and Royle 2015, 2020). This detection probability is likely to play a role in the scaling patterns observed here, especially for the spatial grains resulting from spatial aggregation, as the detection of a species is likely to increase with repeated visits. Thus, we see an opportunity for future assessment of the scaling of species detection probability (Hurlbert and Jetz 2007, Valdez et al. 2023).

Macroecological and practical implications

The difference between $\overline{\Delta S}$ at large and small grains confirms the notion of Sax and Gaines (2003, also see Vellend et al. 2013, Dornelas et al. 2014, Jarzyna and Jetz 2018, Chase et al. 2019 for empirical demonstrations) that temporal trends of biodiversity at large grains (i.e. regional, national or continental) do not reflect biodiversity dynamics at local scale, and vice-versa. We show that this is because extinction and colonization have a different and non-linear relationship between local and larger grains (Fig. 4b, 5b–c,

Yan et al. 2022). This means that, practically, ΔS should be always assessed for a range of grains.

Conclusion

Although we know that spatial scale influences biodiversity change, mechanisms driving this scale-dependency are complex. Here, we highlight, for the first time, how the spatial scaling of colonization, extinction, recurrence, and their respective probabilities play out to drive the scaling of temporal changes of biodiversity. For the Czech avifauna, we show that richness change is more likely to increase at larger grains due to a constantly increasing colonization (indicating colonization from an external species pool) and a hump-shaped scaling of extinction (indicating simultaneous extinction of rare species and decline of common species). These findings appear constant in time (i.e. for the two periods considered), and in space (the same patterns have been found in the literature, Jarzyna and Jetz 2018, Chase et al. 2019). Also, we show that the variation of colonization (not extinction) in time is the main mechanism driving the magnitude of biodiversity change with area for birds of Czechia. This decomposition of richness change through scale is crucial to understand which mechanisms are the most driving the biodiversity changes from local to national and eventually, global scales.

Author contributions

François Leroy: Conceptualization (equal); Formal analysis (lead); Investigation (lead); Methodology (equal); Visualization (lead); Writing – original draft (lead); Writing – review and editing (lead). **Jiří Reif**: Conceptualization (supporting); Data curation (lead); Supervision (supporting); Validation (supporting); Writing – original draft (supporting). **Zdeněk Vermouzek**: Data curation (lead); Validation (supporting); Writing – original draft (supporting). **Karel Šťastný**: Data curation (lead); Writing – original draft (supporting). **Eva Trávníčková**: Data curation (supporting). **Vladimír Bejček**: Data curation (supporting). **Ivan Mikuláš**: Data curation (supporting). **Petr Keil**: Conceptualization (equal); Formal analysis (supporting); Funding acquisition (lead); Investigation (supporting); Methodology (equal); Project administration (lead); Resources (lead); Supervision (lead); Validation (lead); Writing – original draft (supporting); Writing – review and editing (supporting).

Transparent peer review

The peer review history for this article is available at https://publons.com/publon/10.1111/ecog.06995.

Data availability statement

Data are available from the Zenodo repository: https://doi.org/10.5281/zenodo.8432090 (Leroy et al. 2023b).

Supporting information

The Supporting information associated with this article is available with the online version.

References

Adler, P. B. and Lauenroth, W. K. 2003. The power of time: spatiotemporal scaling of species diversity. – Ecol. Lett. 6: 749–756.

Arrhenius, O. 1921. Species and area. – J. Ecol. 9: 95–99.

Barnosky, A. D., Matzke, N., Tomiya, S., Wogan, G. O. U., Swartz, B., Quental, T. B., Marshall, C., McGuire, J. L., Lindsey, E. L., Maguire, K. C., Mersey, B. and Ferrer, E. A. 2011. Has the Earth's sixth mass extinction already arrived? – Nature 471: 7336.

Blowes, S. A. et al. 2019. The geography of biodiversity change in marine and terrestrial assemblages. – Science 366: 339–345.

Breiman, L. 2001. Random forests. – Mach. Learn. 45: 5–32.

Butchart, S. H. M., Stattersfield, A. J., Bennun, L. A., Shutes, S. M., Akçakaya, H. R., Baillie, J. E. M., Stuart, S. N., Hilton-Taylor, C. and Mace, G. M. 2004. Measuring global trends in the status of biodiversity: red list indices for birds. – PLoS Biol. 2: e383.

Cardinale, B. J., Gonzalez, A., Allington, G. R. H. and Loreau, M. 2018. Is local biodiversity declining or not? A summary of the debate over analysis of species richness time trends. – Biol. Conserv. 219: 175–183.

Ceballos, G., Ehrlich, P. R. and Raven, P. H. 2020. Vertebrates on the brink as indicators of biological annihilation and the sixth mass extinction. – Proc. Natl Acad. Sci. USA 117: 13596–13602.

Chase, J. M. et al. 2019. Species richness change across spatial scales. – Oikos 128: 1079–1091.

Chen, T. and Guestrin, C. 2016. XGBoost: a scalable tree boosting system. – In: Proceedings of the 22nd ACM SIGKDD international conference on knowledge discovery and data mining, pp. 785–794.

Chen, T., He, T., Benesty, M., Khotilovich, V., Tang, Y., Cho, H., Chen, K., Mitchell, R., Cano, I., Zhou, T., Li, M., Xie, J., Lin, M., Geng, Y., Li, Y. and Yuan, J. 2022. xgboost: extreme gradient Boosting. – https://CRAN.R-project.org/package=xgboost.

Davey, C. M., Chamberlain, D. E., Newson, S. E., Noble, D. G. and Johnston, A. 2012. Rise of the generalists: evidence for climate driven homogenization in avian communities. – Global Ecol. Biogeogr. 21: 568–578.

Devictor, V., Julliard, R., Clavel, J., Jiguet, F., Lee, A. and Couvet, D. 2008. Functional biotic homogenization of bird communities in disturbed landscapes. – Global Ecol. Biogeogr. 17: 252–261.

Dornelas, M., Gotelli, N. J., McGill, B., Shimadzu, H., Moyes, F., Sievers, C. and Magurran, A. E. 2014. Assemblage time series

reveal biodiversity change but not systematic loss. – Science 344: 296–299.

Dornelas, M., Chase, J. M., Gotelli, N. J., Magurran, A. E., McGill, B. J., Antão, L. H., Blowes, S. A., Daskalova, G. N., Leung, B., Martins, I. S., Moyes, F., Myers-Smith, I. H., Thomas, C. D. and Velland, M. 2023. Looking back on biodiversity change: lessons for the road ahead. – Philos. Trans. R. Soc. Lond. B 378: 20220199.

Finderup Nielsen, T., Sand-Jensen, K., Dornelas, M. and Bruun, H. H. 2019. More is less: net gain in species richness, but biotic homogenization over 140 years. – Ecol. Lett. 22: 1650–1657.

Friedman, J. H. 2001. Greedy function approximation: a gradient boosting machine. – Ann. Stat. 29: 1189–1232.

García-Navas, V., Sattler, T., Schmid, H. and Ozgul, A. 2020. Temporal homogenization of functional and beta diversity in bird communities of the Swiss Alps. – Divers. Distrib. 26: 900–911.

Greenwell, B., Boehmke, B., Cunningham, J. and Developers, G. B. M. 2020. gbm: generalized boosted regression models. – https://CRAN.R-project.org/package=gbm.

Harfoot, M. B. J., Johnston, A., Balmford, A., Burgess, N. D., Butchart, S. H. M., Dias, M. P., Hazin, C., Hilton-Taylor, C., Hoffmann, M., Isaac, N. J. B., Iversen, L. L., Outhwaite, C. L., Visconti, P. and Geldmann, J. 2021. Using the IUCN red list to map threats to terrestrial vertebrates at global scale. – Nat. Ecol. Evol. 5: 1510–1519.

Hastie, T., Tibshirani, R. and Friedman, J. 2009. The elements of statistical learning. – Springer.

Hastings, A., Cuddington, K., Davies, K. F., Dugaw, C. J., Elmendorf, S., Freestone, A., Harrison, S., Holland, M., Lambrinos, J., Malvadkar, U., Melbourne, B. A., Moore, K., Taylor, C. and Thomson, D. 2005. The spatial spread of invasions: new developments in theory and evidence. – Ecol. Lett. 8: 91–101.

Hurlbert, A. H. and Jetz, W. 2007. Species richness, hotspots, and the scale dependence of range maps in ecology and conservation. – Proc. natl Acad. Sci. USA 104: 13384–13389.

Jarzyna, M. A., Zuckerberg, B., Porter, W. F., Finley, A. O. and Maurer, B. A. 2015. Spatial scaling of temporal changes in avian communities: scale dependence of community turnover. – Global Ecol. Biogeogr. 24: 1236–1248.

Jarzyna, M. A. and Jetz, W. 2018. Taxonomic and functional diversity change is scale dependent. – Nat. Commun. 9: 2565.

Keil, P. and Chase, J. M. 2019. Global patterns and drivers of tree diversity integrated across a continuum of spatial grains. – Nat. Ecol. Evol. 3: 390–399.

Keil, P. and Chase, J. M. 2022. Interpolation of temporal biodiversity change, loss, and gain across scales: a machine learning approach. – EcoEvoRxiv, https://doi.org/10.32942/OSF.IO/RKY7B

Keil, P., Biesmeijer, J. C., Barendregt, A., Reemer, M. and Kunin, W. E. 2011. Biodiversity change is scale-dependent: an example from Dutch and UK hoverflies (Diptera, Syrphidae). – Ecography 34: 392–401.

Keil, P., Schweiger, O., Kühn, I., Kunin, W. E., Kuussaari, M., Settele, J., Henle, K., Brotons, L., Pe'er, G., Lengyel, S., Moustakas, A., Steinicke, H. and Storch, D. 2012. Patterns of beta diversity in Europe: the role of climate, land cover and distance across scales. – J. Biogeogr. 39: 1473–1486.

Keil, P., Pereira, H. M., Cabral, J. S., Chase, J. M., May, F., Martins, I. S. and Winter, M. 2018. Spatial scaling of extinction rates: theory and data reveal nonlinearity and a major upscaling and downscaling challenge. – Global Ecol. Biogeogr. 27: 2–13.

Keller, V., Herrando, S., Voříšek, P., Franch, M., Kipson, M., Milanesi, P., Martí, D., Anton, M., Klvaňová, A., Kalyakin, M. V., Bauer, H.-G. and Foppen, R. P. B. 2020. European breeding bird Atlas 2: distribution, abundance and change. – Lynx Edicions.

Kéry, M. and Royle, J. A. 2015. Applied hierarchical modeling in ecology: analysis of distribution, abundance and species richness in R and BUGS: Vol. 1: Prelude and Static Models. – Academic Press.

Kéry, M. and Royle, J. A. 2020. Applied hierarchical modeling in ecology: analysis of aistribution, abundance and apecies richness in R and BUGS: Vol. 2: Dynamic and Advanced Models. – Academic Press.

Koleček, J., Reif, J., Šťastný, K. and Bejček, V. 2010. Changes in bird distribution in a Central European country between 1985–1989 and 2001–2003. – J. Ornithol. 151: 923–932.

Koschová, M., Rivas-Salvador, J. and Reif, J. 2018. Continent-wide test of the efficiency of the European Union's conservation legislation in delivering population benefits for bird species. – Ecol. Indic. 85: 563–569.

Kunin, W. E. 1997. Sample shape, spatial scale and species counts: implications for reserve design. – Biol. Conserv. 82: 369–377.

Leroy, F., Reif, J., Storch, D. and Keil, P. 2023a. How has bird biodiversity changed over time? A review across spatio-temporal scales. – Basic Appl. Ecol. 69: 26–38.

Leroy, F., Reif, J., Vermouzek, Z., Šťastný, K., Trávníčková, E., Bejček, V., Mikuláš, I. and Keil, P. 2023b. Data from: Decomposing biodiversity change to processes of extinction, colonization, and recurrence across scales. – Zenodo Repository, https://doi.org/10.5281/zenodo.8432090 .

MacArthur, R. H. and Wilson, E. O. 1967. The theory of island biogeography. The theory of island biogeography. – Princeton Univ. Press.

MacKenzie, D. I., Nichols, J. D., Royle, J. A., Pollock, K. H., Bailey, L. L. and Hines, J. E. 2006. – Occupancy estimation and modeling: inferring patterns and dynamics of species occurrence. – Elsevier.

May, R. M. 1975. Patterns of species abundance and diversity.

McGill, B. J., Dornelas, M., Gotelli, N. J. and Magurran, A. E. 2015. Fifteen forms of biodiversity trend in the Anthropocene. – Trends Ecol. Evol. 30: 104–113.

McGlinn, D. J., Xiao, X., May, F., Gotelli, N. J., Engel, T., Blowes, S. A., Knight, T. M., Purschke, O., Chase, J. M. and McGill, B. J. 2019. Measurement of Biodiversity (MoB): a method to separate the scale-dependent effects of species abundance distribution, density, and aggregation on diversity change. – Methods Ecol. Evol. 10: 258–269.

Meyer, C., Kreft, H., Guralnick, R. and Jetz, W. 2015. Global priorities for an effective information basis of biodiversity distributions. – Nat. Commun. 6: 8221.

Pereira, H. M., Navarro, L. M. and Martins, I. S. 2012. Global biodiversity change: the bad, the good, and the unknown. – Annu. Rev. Environ. Resour. 37: 25–50.

Pichler, M. and Hartig, F. 2023. Machine learning and deep learning – a review for ecologists. – Methods Ecol. Evol. 14: 994–1016.

Preston, F. W. 1960. Time and space and the variation of species. – Ecology 41: 611–627.

Reif, J., Prylová, K., Šizling, A. L., Vermouzek, Z., Šťastný, K. and Bejček, V. 2013. Changes in bird community composition in the Czech Republic from 1982 to 2004: increasing biotic

homogenization, impacts of warming climate, but no trend in species richness. – J. Ornithol. 154: 359–370.

Reif, J., Szarvas, F. and Šťastný, K. 2021. 'Tell me where the birds have gone' – reconstructing historical influence of major environmental drivers on bird populations from memories of ornithologists of an older generation. – Ecol. Indic. 129: 107909.

Reif, J., Skálová, A. J., Vermouzek, Z. and Voříšek, P. 2022. Long-term trends in forest bird populations reflect management changes in Central European forests. – Ecol. Indic. 141: 109137.

Sauer, J. R., Pardieck, K. L., Ziolkowski, D. J., Jr., Smith, A. C., Hudson, M.-A. R., Rodriguez, V., Berlanga, H., Niven, D. K. and Link, W. A. 2017. The first 50 years of the North American Breeding bird Survey. – Condor 119: 576–593.

Sax, D. F. and Gaines, S. D. 2003. Species diversity: from global decreases to local increases. – Trends Ecol. Evol. 18: 561–566.

Schipper, A. M. et al. 2016. Contrasting changes in the abundance and diversity of North American bird assemblages from 1971 to 2010. – Global Change Biol. 22: 3948–3959.

Šťastný K, Bejček V, Hudec K (1997) Atlas hnízdního rozšíření ptáků v České republice 1985-1989. [Atlas of breeding bird distribution in the Czech Republic 1985-1989]. H & H, Jinočany, 457 pp.

Šťastný K, Bejček V, Hudec K (2006) Atlas hnízdního rozšíření ptáků v České republice: 2001-2003. [Atlas of breeding bird distribution in the Czech Republic: 2001-2003]. Aventinum, Praha, 464 pp.

Šťastný K, Bejček V, Mikuláš I, Telenský T (2021) Atlas hnízdního rozšíření ptáků v České republice 2014-2017. [Atlas of distributions of breeding birds of the Czech Republic 2014-2017]. Aventinum. Praha, 512 pp.

Storch, D. 2016. The theory of the nested species–area relationship: geometric foundations of biodiversity scaling. – J. Veg. Sci. 27: 880–891.

Storch, D., Marquet, P. and Brown, J. (eds) 2007. Scaling biodiversity. – Cambridge Univ. Press.

Storch, D., Koleček, J., Keil, P., Vermouzek, Z., Voříšek, P. and Reif, J. 2023. Decomposing trends in bird populations: climate, life histories and habitat affect different aspects of population change. – Divers. Distrib. 29: 572–585.

Szabo, J. K., Khwaja, N., Garnett, S. T. and Butchart, S. H. M. 2012. Global patterns and drivers of avian extinctions at the species and subspecies level. – PLoS One 7: e47080.

Tilman, D. 1994. Competition and biodiversity in spatially structured habitats. – Ecology 75: 2–16.

Vaidyanathan, G. 2021. The world's species are playing musical chairs: how will it end? – Nature 596: 22–25.

Valdez, J. W., Callaghan, C. T., Junker, J., Purvis, A., Hill, S. L. L. and Pereira, H. M. 2023. The undetectability of global biodiversity trends using local species richness. – Ecography 2023: e06604.

Vellend, M., Baeten, L., Myers-Smith, I. H., Elmendorf, S. C., Beauséjour, R., Brown, C. D., De Frenne, P., Verheyen, K. and Wipf, S. 2013. Global meta-analysis reveals no net change in local-scale plant biodiversity over time. – Proc. Natl Acad. Sci. USA 110: 19456–19459.

Wilson, R. J., Thomas, C. D., Fox, R., Roy, D. B. and Kunin, W. E. 2004. Spatial patterns in species distributions reveal biodiversity change. – Nature 432: 7015.

Wilting, H. C., Schipper, A. M., Bakkenes, M., Meijer, J. R. and Huijbregts, M. A. J. 2017. Quantifying biodiversity losses due to human consumption: a global-scale footprint analysis. – Environ. Sci. Technol. 51: 3298–3306.

Wright, M. N. and Ziegler, A. 2017. ranger: a fast implementation of random forests for high dimensional data in C++ and R. – J. Stat. Softw. 77: 1–17.

Yan, C., He, F., He, J. and Zhang, Z. 2022. The relationship between local and regional extinction rates depends on species distribution patterns. – Ecography 2022.